IEEE Access
Multidisciplinary | Rapid Review | Open Access Journal

Received November 6, 2020, accepted November 10, 2020, date of publication November 17, 2020,
date of current version December 1, 2020.

Digital Object Identifier 10.1109/ACCESS.2020.3038553

Discrimination of Verbal/Visuospatial Memory Retrieval Processes by Measuring Prefrontal Lobe Blood Volume With Functional Near-Infrared Spectrometry

YOSUKE KURIHARA[1], (Member, IEEE), TAKASHI KABURAGI[2], (Member, IEEE), KEITA NISHIO[1], YURI HAMADA[1], (Member, IEEE), TOSHIYUKI MATSUMOTO[1], AND SATOSHI KUMAGAI[1]

[1]Department of Industrial and Systems Engineering, Aoyama Gakuin University, Sagamihara 2525258, Japan
[2]Department of Natural Sciences, International Christian University, Tokyo 181-8585, Japan

Corresponding author: Yosuke Kurihara (kurihara@ise.aoyama.ac.jp)

ABSTRACT In cognitive task execution, retrieval processes transfer memories from long-term storage to working memory, comprising three short-term memories—phonological loop, visuospatial sketchpad, and episodic buffer—controlled by a short-term-memory central executive. The phonological loop and visuospatial sketchpad are prominent in verbal and visuospatial information processing, respectively. Individuals differ in how they retrieve the same information. Discrimination between verbal or visuospatial memory retrieval by monitoring central executive activation is useful. Functional near-infrared spectroscopy (fNIRS) was used to assess blood volume and prefrontal lobe brain activation. Using a novel approach, blood volume during memory retrieval was obtained using fNIRS. To eliminate other factors not related to the central executive activation, a base period was observed. Dynamic range was calculated for both memory retrieval and base periods, and differences obtained at ten positions within the prefrontal lobe were used as features to discriminate between verbal and visuospatial retrieval. For discrimination, k-nearest neighbor (kNN) and support vector machine (SVM) with different kernels were applied. Our method was tested on participants in verbal/visuospatial memory retrieval experiments. As the result, accuracy, positive predictive values, and negative predictive values of kNN and SVM were 1, which indicated that the proposed method successfully discriminated between verbal/visuospatial memory retrieval through prefrontal lobe blood volume observation.

INDEX TERMS k-nearest neighbor, memory retrieval, fNIRS, support vector machine, working memory.

I. INTRODUCTION

Memory retrieval refers to the process of accessing past experiences or information that has been previously encoded and stored in the brain. During the execution of cognitive tasks, retrieval processes transfer memories from long-term storage to working memory. The relationship between memory and brain activation has been studied in numerous contexts [1]–[25]. A functional working memory model has been proposed in [1] and revised in [2]–[5], and many researchers now use the revised model [4]. The primary concept underlying the model is that an operating system called the central executive controls three short-term memory systems: the phonological loop, visuospatial sketchpad, and episodic buffer. Among these, the phonological loop and visuospatial sketchpad play prominent roles in verbal information and visuospatial information processing [4], [6], [7], respectively. The relationship between verbal and visuospatial retrieval and brain activities, including working memory, has also been experimentally researched [26]–[30]. Here, there are individual differences in whether the same information is retrieved verbally or visuospatially. Thus, it is useful to be able to discriminate between whether a person verbally or visuospatially retrieves memories by monitoring

The associate editor coordinating the review of this manuscript and approving it for publication was Yuan-Pin Lin.

the phonological loop and the visuospatial sketchpad activation. This knowledge can aid in developing suitable teaching materials or generating strategies for student-centered teaching in the field of education. However, monitoring both the phonological loop and visuospatial sketchpad activation requires monitoring two different parts of the brain with multiple sensors. Positioning such sensors precisely on the head would be uncomfortable for the participant. Thus, instead of monitoring both the activation of the phonological loop and the visuospatial sketchpad, here, only the central executive activation is considered for monitoring, which controls the phonological loop and visuospatial sketchpad.

Recent studies have evaluated brain activity using electroencephalography (EEG) [14], [19], [23], functional magnetic resonance imaging (fMRI) [11], [13], [16], [24], [31], functional near-infrared spectroscopy (fNIRS) [15], [17], [18], [21], [22], [32]–[36], and positron emission tomography (PET) [25]. Although fMRI and PET systems have high spatial resolution, they require a special operating environment, such as a magnetically shielded room. In contrast, although EEG and fNIRS have low spatial resolution, they can measure brain activity in normal environments such as the home. Furthermore, these approaches are noninvasive and less restrictive in terms of patient comfort. The EEG is sensitive to myoelectric signals generated due to body movements, whereas fNIRS is insensitive and robust to myoelectric signals and therefore can be used in conjunction with wearable devices. Thus, fNIRS may be particularly suitable for measuring brain activation. Furthermore, the central executive is primarily distributed in the middle prefrontal gyri of the BA46/10, BA9/44, and BA45 areas [12], making the central executive conveniently accessible for fNIRS analysis. Therefore, we know which regions of the brain to focus on when performing verbal/visuospatial memory retrieval discrimination.

In regard to verbal memory retrieval and blood volume measured by fNIRS, Herrmann MJ *et al.* investigated the blood oxygenation changes associated with the execution of the verbal fluency test (VFT) in the left and right prefrontal brain areas [26]. They found a significant increase in oxyhemoglobin (oxy-Hb) and a significant decrease in deoxyhemoglobin (deoxy-Hb) during the execution of the VFT over both hemispheres. Huang *et al*. showed different patterns of brain functional connectivity during the two VFT types, which was consistent with the different cognitive requirements of each task [27]. They demonstrated increased brain functional connectivity over the frontal and temporal regions during the letter fluency task than during the category fluency task. With regard to visuospatial memory retrieval and blood volume measured by fNIRS, Ayaz *et al*. showed that frontal cerebral oxygenation measured by fNIRS increases with the working memory load [28]. Nakahachi *et al*. measured relative changes in the concentration of oxy-Hb in the frontal area using fNIRS during the Advanced Trail Making Test (ATMT), a tool used to assess visuospatial working memory [29]. The ATMT consists of two tasks, and they showed that channel activation of both tasks was observed at different locations. The more ventral lateral regions exhibited more sustained activity during face working memory delays than during spatial working memory delays, whereas the region in the superior frontal sulcus demonstrated more sustained activity during spatial working memory delays. In contrast, the regions in the medial wall showed equivalent levels of sustained activity during both types of visual working memory delays. Furthermore, in research related to blood volume in both verbal and visuospatial memory retrieval, McKendrick *et al.* continuously monitored trainees with fNIRS while they performed a dual verbal–spatial working memory task [30]. They observed nonlinear increases in the left dorsolateral prefrontal cortex and right ventrolateral prefrontal cortex with increased exposure to working memory training. The findings of these studies imply that verbal and visuospatial memory retrieval could be discriminated by observing blood volume.

In [35], [36], the various types of tasks to be discriminated from brain activity measured by fNIRS and the classifier used for task discrimination are comprehensively reviewed. The k-nearest neighbor (kNN) has been proposed as a non-parametric method to discriminate tasks from the brain blood volume measured by fNIRS. Conversely, linear discriminant analysis [33], [34], and threshold-based partial least squares discriminant analysis have been proposed as linear discrimination methods; quadratic discriminant analysis, artificial neural network, support vector machine (SVM) [34], and extreme learning machine as nonlinear discrimination methods; and the hidden Markov model and naïve Bayes classifier as probabilistic discrimination methods. These methods do not discriminate between verbal and visuospatial memory retrieval.

Against this backdrop, in this study, a novel method is proposed that can discriminate between a person retrieving memories verbally or visuospatially by utilizing the measured blood volume via fNIRS to evaluate brain activation in the prefrontal lobe, where the central executive function is located. To eliminate other factors not related to the central executive activation, such as muscle activation, a base period is also observed. The dynamic range is calculated for both the memory retrieval and base periods. The differences in the dynamic ranges obtained at ten positions within the prefrontal lobe are used as features to discriminate between verbal and visuospatial memory retrieval. For discrimination methods, kNN and SVM with different kernels was used. The accuracy, positive predictive values (PPVs), and negative predictive values (NPVs) of kNN and SVM were compared in the verification experiment.

II. PROPOSED METHOD

In this section, a model representing how the central executive affects the blood volume during memory retrieval is proposed along with a signal processing approach that can discriminate between whether a person retrieves memories verbally or visuospatially based on the blood volume

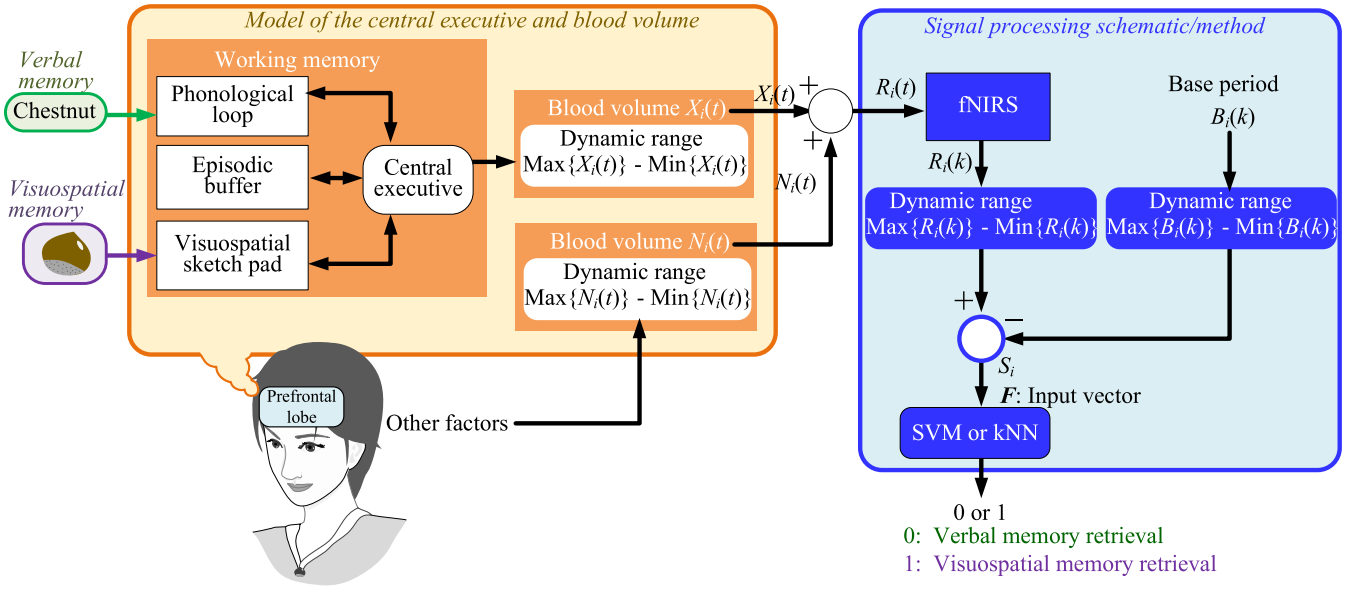

FIGURE 1. Complete relation schematic diagram of the proposed method that consists of a model and our signal processing schematic/method. During memory retrieval, the central executive controls the phonological loop, visuospatial sketch pad, and episodic buffer. This exercise of control is reflected in the dynamic range of the blood volume in the prefrontal lobe (where the central executive is located) and other factors. The blood volume in the prefrontal lobe during verbal or visuospatial memory retrieval is measured via functional near-infrared spectroscopy (fNIRS) for n channels. Indices S_i are calculated from signals $R_i(k)$ and $B_i(k)$. A vector composed of indices S_i is input to the k-nearest neighbor (kNN) or the support vector machine (SVM). Finally, kNN or the SVM discriminates the input vector as 0 (verbal memory retrieval) or 1 (visuospatial memory retrieval).

measured via fNIRS. Fig. 1 shows the complete relation schematic of the model and the signal processing method.

A. MODEL RELATING CENTRAL EXECUTIVE AND BLOOD VOLUME IN PREFRONTAL LOBE DURING MEMORY RETRIEVAL

During the memory retrieval process, the central executive controls the information flow from the phonological loop, visuospatial sketch pad, and episodic buffer [4].

Here, a model is proposed that represents how the operation of the central executive affects the blood volume during memory retrieval. The left panel in Fig. 1 shows the proposed model of the central executive and the corresponding blood volume changes based on memory retrieval. In this study, to construct the model, assumptions (A1) and (A2) are made regarding the central executive and the blood volume.

(A1): Activation of the central executive affects the dynamic range of blood volume during memory retrieval.

(A2): The distribution pattern of the dynamic blood volume range in the prefrontal lobe differs depending on the type of memory retrieval process.

The results of [26], [28], [30] indicate that cerebral blood flow increases or decreases during the recall process, regardless of verbal or visuospatial recall. Therefore, to consider the characteristics, (A1) is assumed. In (A1), the activation of the central executive affects the blood volume during control of information arising due to memory retrieval, particularly the dynamic blood volume range around the prefrontal lobe where the central executive is located. Let $X_i(t)$ $(i = 1, 2, \ldots n)$ be the blood volume with index i, which indicates an anatomical location/position on the prefrontal lobe, and t and n denote continuous time and the total number of locations, respectively, in the prefrontal lobe. Hence, the dynamic range is represented as $\mathrm{Max}\{X_i(t)\} - \mathrm{Min}\{X_i(t)\}$. In addition, the results of [27], [29] indicate that the location in which the cerebral blood flow changes vary depending on verbal and visuospatial recall. Therefore, to consider the characteristics, (A2) is assumed. In (A2) because the working pattern for controlling the information flow of the central executive is different depending on the type of memory retrieval, the distribution pattern of the dynamic range at each location i around the prefrontal lobe also differs depending on the type of memory retrieval. In addition, the blood volume is influenced by other factors not related to the activation of the central executive, such as muscle activation. Let $N_i(t)$ denote the blood volume due to these other factors, which also affect the dynamic range, as $\mathrm{Max}\{N_i(t)\} - \mathrm{Min}\{N_i(t)\}$. Therefore, the blood volume $R_i(t)$, which is observable at location i during memory retrieval, can be represented as $R_i(t) = X_i(t) + N_i(t)$, and the dynamic range $\mathrm{Max}\{R_i(t)\} - \mathrm{Min}\{R_i(t)\}$ can be represented as follows:

$$Max\{R_i(t)\} - Min\{R_i(t)\} = [Max\{X_i(t)\} - Min\{X_i(t)\}] + [Max\{N_i(t)\} - Min\{N_i(t)\}]. \quad (1)$$

B. SIGNAL PROCESSING TO DISCRIMINATE BETWEEN VERBAL AND VISUOSPATIAL MEMORY RETRIEVAL FROM BLOOD VOLUME MEASURED BY fNIRS

In this section, a signal processing flow is proposed that can help discriminate between whether a person retrieves

memories verbally or visuospatially, from the blood volume measured by fNIRS. The right panel in Fig. 1 shows the signal processing schematic/method utilized after obtaining the blood volume using fNIRS.

1) DEFINITION OF INDICES BASED ON DYNAMIC BLOOD VOLUME RANGE

To discriminate memory retrieval based on assumptions (A1) and (A2), the dynamic range $\mathrm{Max}\{X_i(t)\} - \mathrm{Min}\{X_i(t)\}$ is obtained at each location around the central executive, and discrimination between verbal and visuospatial memory retrieval is performed by studying the distribution pattern of the dynamic range in the prefrontal lobe.

To obtain $\mathrm{Max}\{X_i(t)\} - \mathrm{Min}\{X_i(t)\}$, the blood volume $R_i(t)$ is measured, which contains both $X_i(t)$ and $N_i(t)$, via fNIRS. The fNIRS probes were attached to the left and right BA46 regions and the center of the BA10 region of the brain. In the international 10–20 system, these positions correspond to the upper F7-Fpz-F8 line. Hence, the fNIRS probes cover the central executive regions. These probes measure oxy-Hb and deoxy-Hb. Here, oxy-Hb is used as the regional cerebral blood volume of dimension [m(mol/l)mm]. Let $R_i(k)$ be the discrete time series signal of the blood volume measured by fNIRS at n points (channels) on the prefrontal lobe during memory retrieval. Parameter k represents a discrete time period with sampling interval Δt. Because $R_i(k)$ contains both $X_i(k)$ and $N_i(k)$, $\mathrm{Max}\{R_i(k)\} - \mathrm{Min}\{R_i(k)\}$ also includes both $\mathrm{Max}\{X_i(k)\} - \mathrm{Min}\{X_i(k)\}$ and $\mathrm{Max}\{N_i(k)\} - \mathrm{Min}\{N_i(k)\}$. Hence, to obtain $\mathrm{Max}\{X_i(t)\} - \mathrm{Min}\{X_i(t)\}$ from the measured $R_i(k)$, the base period signal $B_i(k)$ is introduced, which can negate the influence of $N_i(k)$. Next, the indices S_i are defined as follows:

$$S_i = [Max\{R_i(k)\} - Min\{R_i(k)\}] - [Max\{B_i(k)\} - Min\{B_i(k)\}]. \quad (2)$$

From (1) and (2), when the value of $\mathrm{Max}\{B_i(k)\} - \mathrm{Min}\{B_i(k)\}$ approximates $\mathrm{Max}\{N_i(k)\} - \mathrm{Min}\{N_i(k)\}$, the indices S_i also approximate $\mathrm{Max}\{X_i(k)\} - \mathrm{Min}\{X_i(k)\}$. The indices S_i were obtained at n points on the prefrontal lobe. These are the indices that correspond to assumption (A1) in the signal processing approach.

2) METHODS FOR DISCRIMINATING BETWEEN VERBAL AND VISUOSPATIAL MEMORY RETRIEVAL

To discriminate between verbal and visuospatial memory retrieval via the distribution pattern of S_i at each location, a discrimination method was applied. Let $\boldsymbol{F} = [S_1, S_2 \ldots S_n]^T$ be an input vector for the discrimination method and y be a function that receives the input vector $\boldsymbol{F}$. Let 0 and 1 be labels for verbal memory retrieval and visuospatial memory retrieval, respectively. The output of y is 0 for verbal memory retrieval and 1 for visuospatial memory retrieval. The kNN and SVM are compared as discrimination methods. In the kNN case, y is expressed in (3), where k_{nn} denotes the number of training data nearest to the test data for kNN:

$$y = \begin{cases} 0, & if\ k_{nn} - nearest\ neighbor\ (s)\ are\ 0 \\ 1, & if\ k_{nn} - nearest\ neighbor\ (s)\ are\ 1 \end{cases} \quad (3)$$

In the case of the SVM, y is expressed as follows:

$$y = \begin{cases} 0, & f(\boldsymbol{F}) < 0\ (Verbal\ memory\ retrieval) \\ 1, & f(\boldsymbol{F}) \geq 0\ (Visuospatial\ memory\ retrieval) \end{cases}, \quad (4)$$

$$f(\boldsymbol{F}) = \sum_{j=1}^{N_s} \alpha_j y_j K\left(\boldsymbol{F}^T \boldsymbol{F}_j\right) + b. \quad (5)$$

The parameter N_s in (5) represents the total number of support vectors. The Lagrange multiplier α and bias b are calculated by means of an optimization that maximizes the soft margin. Further, $K(\boldsymbol{F}^{\mathrm{T}}\boldsymbol{F}_j)$ in (5) denotes an SVM kernel. The application of the SVM to S_i distributed around the prefrontal lobe to discriminate between verbal or visuospatial memory retrieval is the processing that corresponds to the (A2) assumption in the signal processing approach.

III. VERIFICATION EXPERIMENTS

To verify the feasibility of the proposed method, verification experiments were conducted.

A. EXPERIMENTAL PROCEDURES

The experiments consisted of a verbal memory retrieval experiment and a visuospatial memory retrieval experiment.

1) VERBAL MEMORY RETRIEVAL EXPERIMENT

The verbal memory retrieval experiment needed to produce only verbal memory retrieval; accordingly, a VFT [37] that has been utilized in studies was used to assess the relationship between verbal function and brain activity [26], [27], [38]–[43]. In the experiment, one letter was presented to participants, who were required to generate as many words as possible in a given time interval that began with the letter presentation. The blood volume measured by fNIRS during the VFT contained not only a memory retrieval component but also a verbalization component.

Fig. 2 shows the experimental paradigm for the verbal retrieval experiment. At the start of the experiment, the experimenter instructed the participant to perform the experimental procedure and attached the headset for fNIRS measurement to the participant. The participant was asked to rest for some time as a mental preparation while the experimenter began the fNIRS measurement. After the baseline fNIRS was calibrated for 10 s during the participant's rest period, recording of blood volume began. To measure the blood volume associated with brain activation due to verbalization, each participant was asked to repeatedly produce meaningless sounds for 60 s. The recording over the last 10 s was used as the base period signal $B_i(k)$. Next, the participant was asked to work on the VFT. One letter was presented to the participants, who generated words that began with this letter for 20 s as one trial

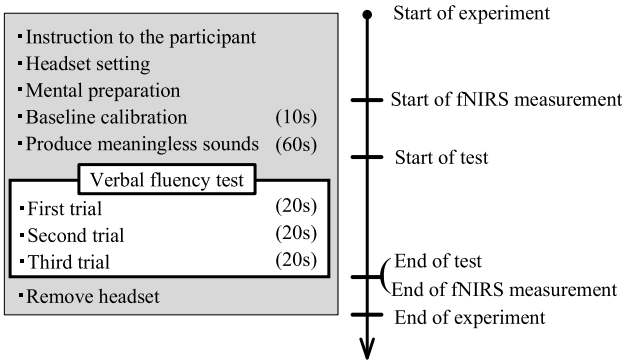

FIGURE 2. Experimental paradigm for the verbal retrieval experiment.

because the preliminary research showed that participants could continuously retrieve words throughout the 20 s. The participants repeated the trial three times; therefore, the total test time was 60 s. Different letters were applied for each trial. The VFT and fNIRS measurements were completed after the third trial. The signal obtained over this 60-s period was defined as the retrieval period signal $R_i(k)$. The experimenter then removed the headset from the participant and ended the verbal retrieval experiment.

2) VISUOSPATIAL MEMORY RETRIEVAL EXPERIMENT

The visuospatial memory retrieval experiment was required to produce only visuospatial memory retrieval. Accordingly, the Rey–Osterrieth complex figure (ROCF) test was used [44]. This test has been used in studies that aim to assess visuospatial memory [45]–[51]. Fig. 3 shows the complex figure used in the test.

Fig. 4 shows the experimental paradigm for the visuospatial retrieval experiment. The experimental procedures performed before the ROCF test are the same as those performed in the verbal retrieval experiment. Next, the participant was asked to work on the ROCF test. To measure brain activation artifacts associated with drawing the figure, participants were required to copy a complex figure. The blood volume during copying was measured by fNIRS, and the last 10 s of the measured signal was defined as the base period signal $B_i(k)$. After copying the figure, the participants waited for 3 min. After the 3-min period, the participants drew the same figure, but from memory this time. A time limit of 60 s was imposed, and the blood volume signal produced over this period was defined as $R_i(k)$. The experimenter removed the headset from the participant, which ended the visuospatial retrieval experiment.

In the verification experiment, it was preferable that the participant performed only recall during the measurement. In the ROCF test, the measurement time was set to 60 s because it was known from the preliminary experiment that it would take more than 60 s. In the VFT, the test duration was set to three trials for 60 s because it was known from the previous experiment that participants always recall the

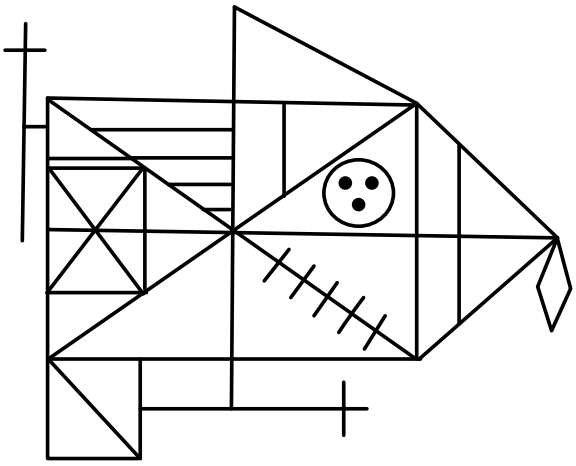

FIGURE 3. Rey–Osterrieth complex figure for the visuospatial memory retrieval experiment. In this experiment, participants are required to copy a complex figure to measure brain activation artifacts associated with drawing the figure, and the blood volume is measured by fNIRS. After copying the figure, the participants wait for 3 min. After the 3-min period, the participants are required to draw the same figure from memory without seeing the complex figure.

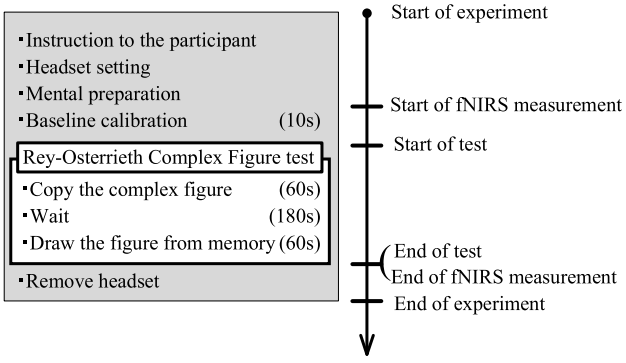

FIGURE 4. Experimental paradigm for the visuospatial retrieval experiment.

information within 20 s. If the number of trials was smaller than that, recall would be delayed, which was not ideal.

B. SETUP FOR VERIFICATION EXPERIMENTS AND PARTICIPANTS

In the experiment, the WOT-100 fNIRS setup by Hitachi Co. was used for fNIRS measurements; Fig. 5 shows the sensor locations. This wearable headset device has 10 channel probes (i.e., the number of points on the prefrontal lobe n is 10 in this experiment) that cover the right and left BA46 and BA10 regions. In this study, all of the detection points were set to prevent any interference due to hair. The array of lower probes measuring channels 3, 6, and 9 was positioned along the F7-Fpz-F8 line of the international 10–20 system. Channels 1–3, 4–7, and 8–10 cover BA46 (right), BA10, and BA46 (left), respectively. This wearable headset device measures both oxy-Hb and deoxy-Hb. In this experiment, the oxy-Hb was used as the blood volume. The sampling interval Δt was set to 0.2 s. Fig. 6 shows the experimental environment. The experiment was conducted in an ordinary

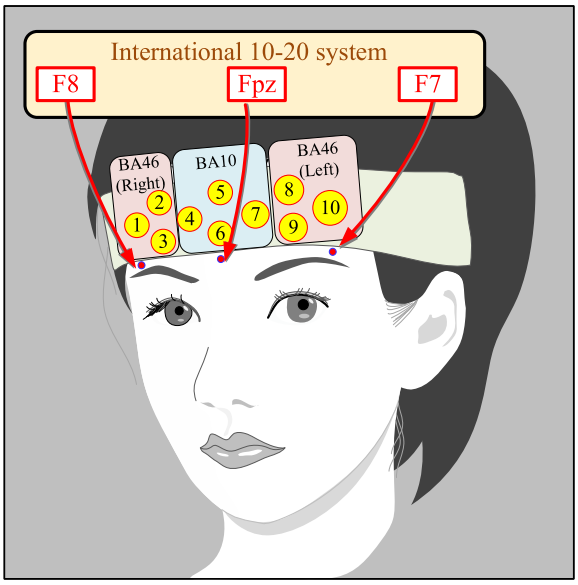

FIGURE 5. Sensor locations (10 channels) for assessment of prefrontal blood volume by functional near-infrared spectroscopy (fNIRS) topography that cover the right and left BA46 as well as BA10 regions. All of the detection points are set to prevent interference due to hair. The array of lower probes measuring channels 3, 6, and 9 is positioned along the F7-Fpz-F8 line of the international 10–20 system. Channels 1–3, 4–7, and 8–10 cover BA46 (right), BA10, and BA46 (left), respectively. Ten indices S1, S2, . . . , S10 are calculated from the blood volume measured at the 10 abovementioned points for each participant.

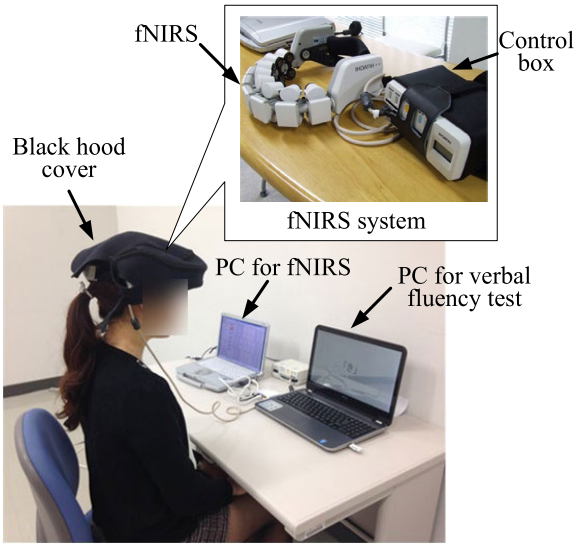

FIGURE 6. Environment used for verification experiments. The participant wears the functional near-infrared spectroscopy (fNIRS) setup on the prefrontal lobe. The fNIRS is covered by a black hood to prevent interference from environmental light. The fNIRS is connected to the control box, and the measured data are transferred to the PC for the fNIRS. For the verbal memory retrieval experiment, the PC is placed in front of the participant to display one letter.

room that was quiet enough for participants to concentrate on the task. As shown in Fig. 6, the participants wore the fNIRS system, and a black hood was used to cover it to prevent interference from ambient light. The participants were 20 healthy Japanese university engineering students (7 females and 13 males), aged 20 to 23. All experiments were performed in accordance with the program checked and approved by the Life Science Committee of Aoyama Gakuin University (permission No. M15-17). All participants provided informed consent. For all 20 participants, 10 indices S_1, $S_2, \ldots S_{10}$ were calculated for all 10 channels observed, and input vectors $\boldsymbol{F}$ were obtained for the verbal and visuospatial memory retrieval experiments. Hence, a total of 40 input vectors were obtained.

C. EVALUATION METHOD

The results of the discrimination by kNN or SVM were evaluated using a cross-validation method. A 20-fold cross-validation was performed. For each fold, among all 20 participants' 40 input vectors, 19 participants' input vectors $\boldsymbol{F}$, obtained from both verbal and visuospatial memory retrieval experiments (i.e., 38 input vectors), were used for training data. After training the kNN or SVM, one participant's two input vectors $\boldsymbol{F}$, which were not used in training, were used as test data. The above procedure was repeated for all participants. The kNN or SVM discriminated between whether $\boldsymbol{F}$ represented verbal or visuospatial memory retrieval. The discrimination result was considered correct if the discriminated memory retrieval matched the actual memory retrieval. Otherwise, the results of the discriminated memory retrieval were interpreted as incorrect. Finally, the true positive (TP), true negative (TN), false positive (FP), and false negative (FN) values, were aggregated and calculated $Accuracy$, PPV, and NPV were calculated as follows:

$$Accuracy = \frac{TP + TN}{TP + FP + FN + TN}, \tag{6}$$

$$PPV = \frac{TP}{TP + FP}, \tag{7}$$

$$NPV = \frac{TN}{TN + FN}. \tag{8}$$

In our experiments, $k_{nn} = 1, 3, 5$, and 10 was applied for kNN; and linear, quadratic, polynomial, and Gaussian kernels were applied for the SVM. Subsequently, the abovementioned parameters of $Accuracy$, PPV, and NPV were calculated for each k_{nn} and kernel.

IV. EXPERIMENTAL RESULTS

A. TYPICAL RESULTS OF BLOOD VOLUME MEASURED BY fNIRS FOR EACH EXPERIMENT

Figs. 7 to 12 show 10 blood volume signals for three participants, as measured by fNIRS.

Figs. 7 and 8 show typical examples with one participant during verbal and visuospatial memory retrieval experiments. In Fig. 7, the blue line represents the blood volume corresponding to the participant repeatedly producing meaningless sounds for 60 s, and the red line represents the blood volume corresponding to the generation of words with the same initial letter by the participant. The signal in the period from 50 to 60 s is used as the base period signal $B_i(k)$, and

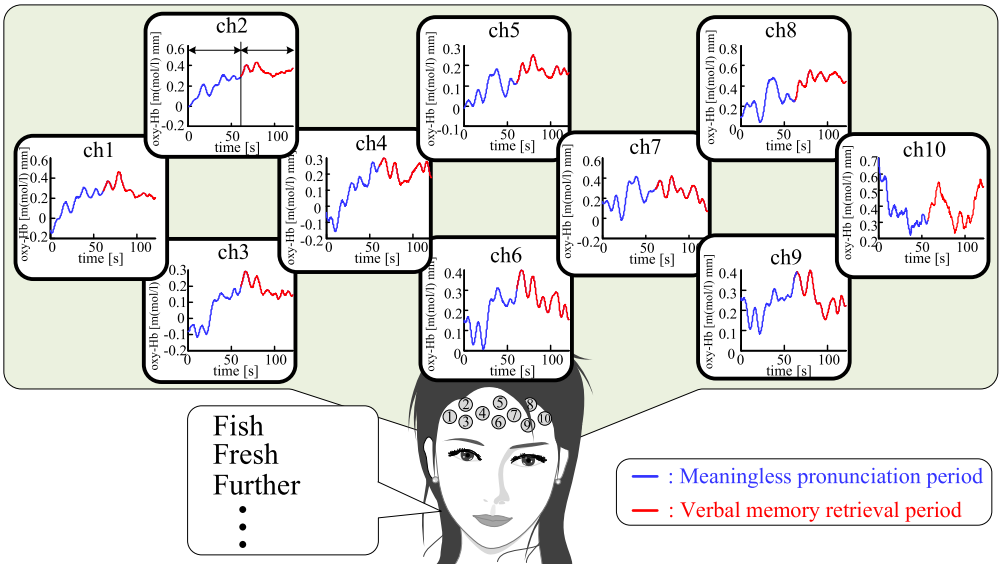

FIGURE 7. Sample blood volume signals measured by functional near-infrared spectroscopy (fNIRS) topography during the verbal memory retrieval experiment. The period from 0 to 60 s, represented by the blue line, shows the blood volume corresponding to the participant repeatedly producing meaningless sounds; and the signal from 50 to 60 s is used as the base period signal $B_i(k)$. After the production of meaningless sounds, the participants generated words whose initial letter was the same as the letter shown on the PC display from 60 to 120 s. The red line, representing the blood volume during the verbal fluency test, is used as the verbal memory retrieval period signal $R_i(k)$.

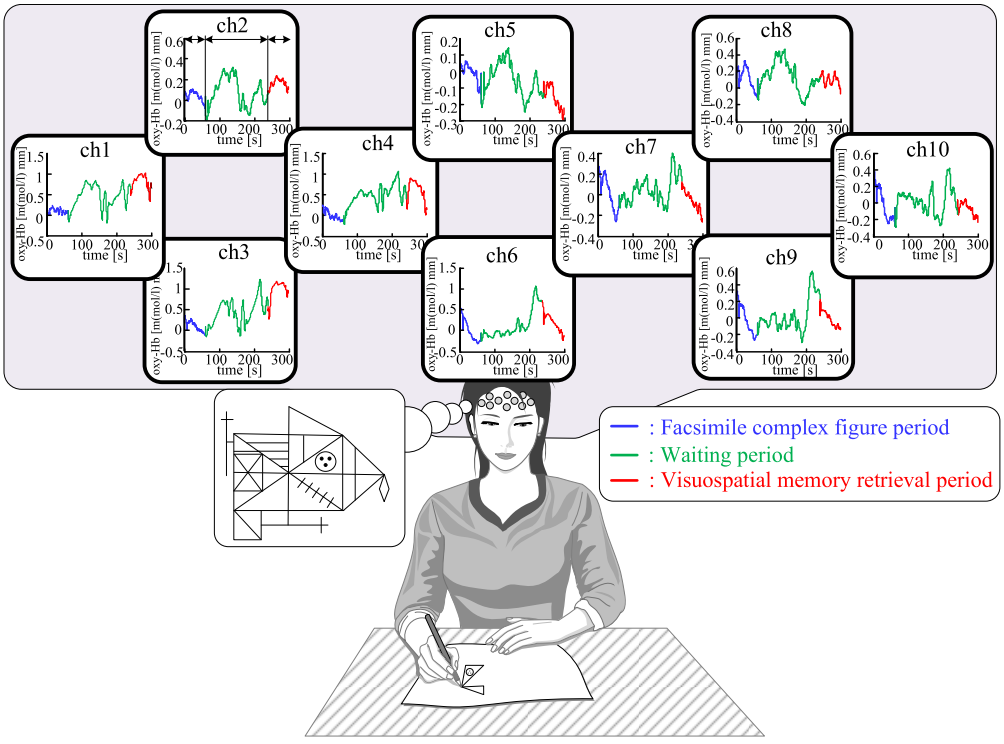

FIGURE 8. Sample blood volume signals measured by functional near-infrared spectroscopy (fNIRS) topography during the visuospatial memory retrieval experiment. In the period from 0 to 60 s, the participant copied the Rey–Osterrieth complex figure. The blue line represents the blood volume during the copying, and the signal of the period from 50 to 60 s is used as the base period signal $B_i(k)$. After copying the figure, the participant waited for 3 min. The waiting period is represented by the green line from 60 to 240 s. From 240 to 300 s, the participant drew the same figure from memory. The red line, which represents the blood volume during the Rey–Osterrieth complex figure test, is used as the visuospatial memory retrieval period signal $R_i(k)$.

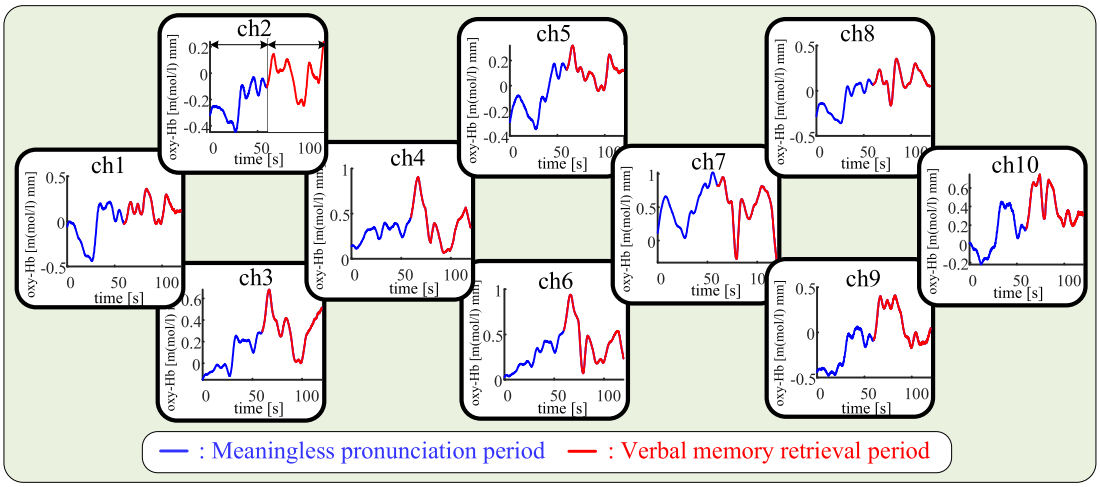

FIGURE 9. Sample blood volume signals of a different participant from that of Figs. 7 and 8 measured by functional near-infrared spectroscopy (fNIRS) topography during the verbal memory retrieval experiment.

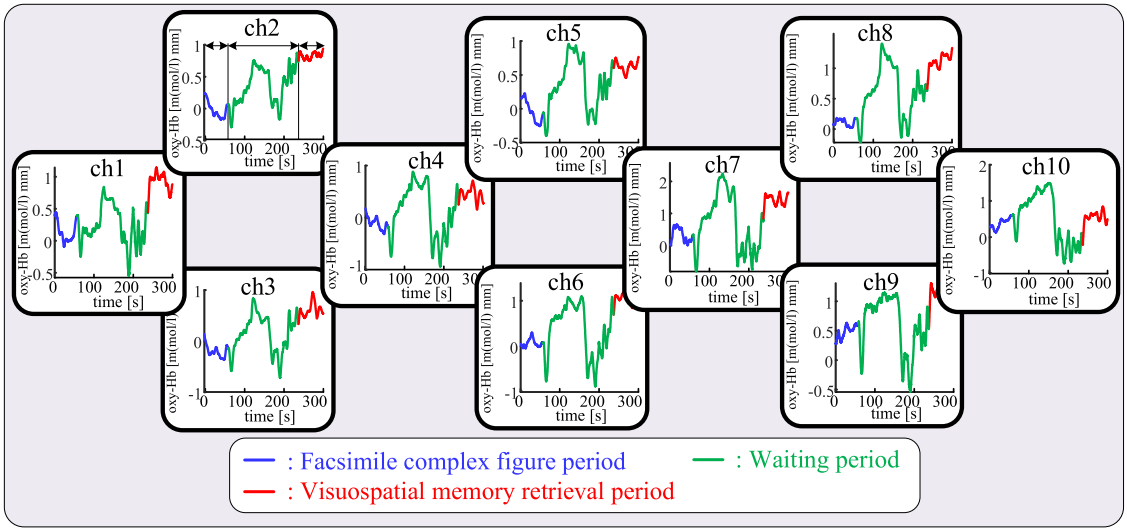

FIGURE 10. Sample blood volume signals of a different participant from that of Figs. 7 and 8 measured by functional near-infrared spectroscopy (fNIRS) topography during the visuospatial memory retrieval experiment.

the period from 60 to 120 s is used as the verbal memory retrieval period signal $R_i(k)$. As shown in Fig. 7, when compared with the 10 measured signals, the amplitudes of the signals during the verbal memory retrieval period are different in each region. The amplitudes of signals from ch1–6, located at the right BA46 and BA10 regions, vary within the range 0.1–0.2. m(mol/l)mm. The signal amplitudes of ch7–10, located on the left BA46 region, vary within the range 0.25–0.4. m(mol/l)mm. In Fig. 8, the blue line represents the blood volume corresponding to the interval when the participant copied the ROCF. The green line represents the volume corresponding to the participant waiting for 3 min, and the red line represents the blood volume corresponding to the participant drawing the same complex figure from memory. The signal from the period of 50 to 60 s is used as the base period signal $B_i(k)$, and that from 240 to 300 s is used as the visuospatial memory retrieval signal $R_i(k)$. As shown in Fig. 8, the 10 measured signals can be classified into two patterns. One pattern is that $R_i(k)$ increases for 30 s after the beginning of drawing and subsequently decreases. This pattern is recorded in ch1–4, located in the right BA46 region. The second pattern is that $R_i(k)$ gradually decreases toward the end of the experiment; this pattern is recorded in ch5–7 and ch9–10, which are located in the BA10 and left BA46 regions, respectively.

Figs. 9 and 10 show typical examples with another participant during verbal and visuospatial memory retrieval experiments. As shown in Fig. 9, the minimum values of $R_i(k)$ are observed at approximately 100 s in the right hemisphere (ch1–5) including BA46 and at approximately 80 s in ch6–8. In addition, the averages of the dynamic range were moderately different, 0.55 m(mol/l)mm for

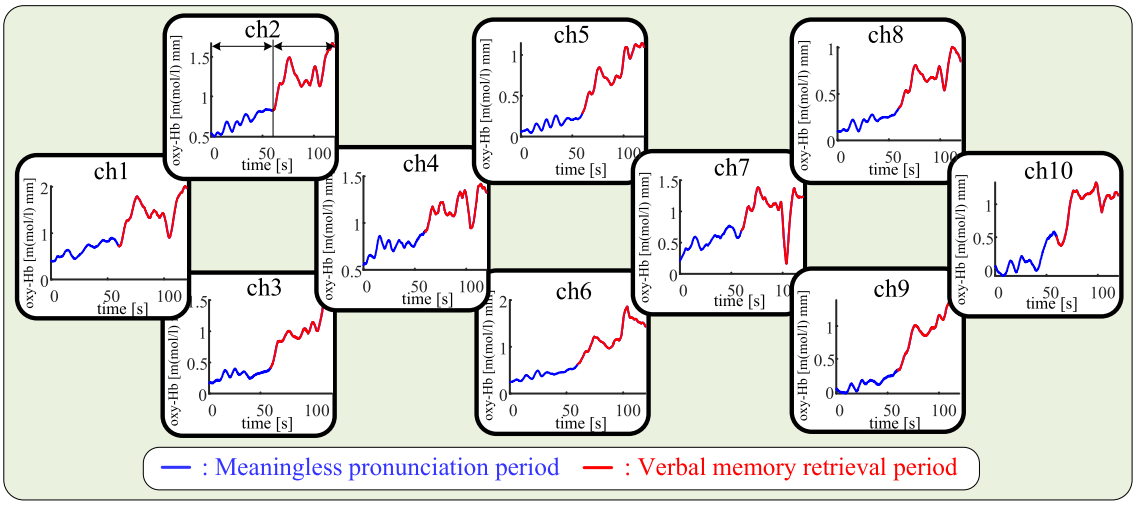

FIGURE 11. Sample blood volume signals of a different participant from that of Figs. 7 and 8 measured by functional near-infrared spectroscopy (fNIRS) topography during the verbal memory retrieval experiment.

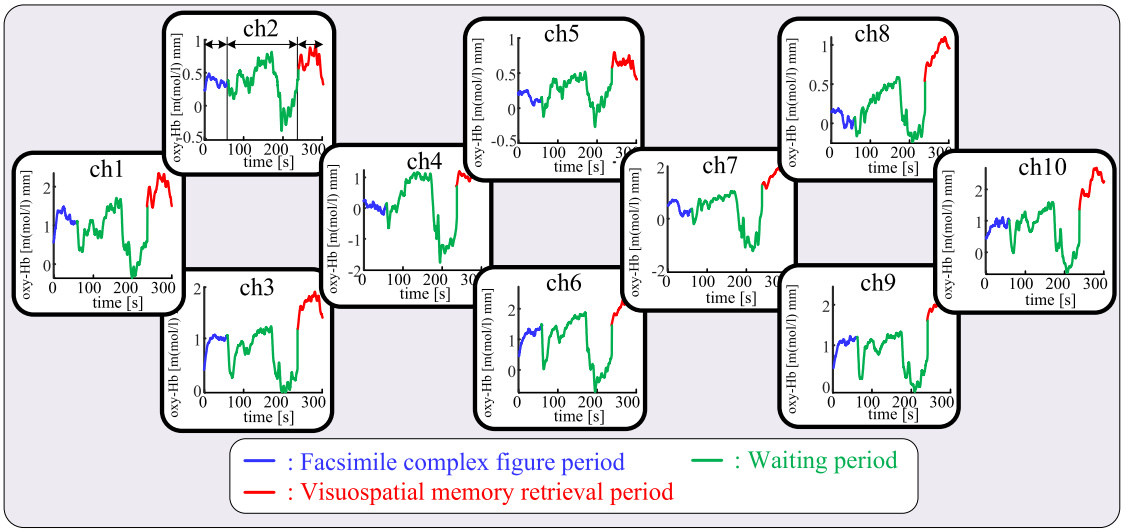

FIGURE 12. Sample blood volume signals of a different participant from that of Figs. 7 and 8 measured by functional near-infrared spectroscopy (fNIRS) topography during the visuospatial memory retrieval experiment.

ch1–5 and 0.89 m(mol/l)mm for ch6–8. In ch1–4 of Fig. 10, $R_i(k)$ increases for 30 s after the beginning of drawing and subsequently decreases, as confirmed in Fig. 7. In this case, this tendency is confirmed in ch5–10 and ch1–4. The average dynamic ranges for ch1–5 and ch6–8 were 0.48 m(mol/l)mm and 0.74 m(mol/l)mm, respectively.

Figs. 11 and 12 show typical examples with another participant during verbal and visuospatial memory retrieval experiments. As shown in Fig. 11, the blood volume $R_i(k)$ tends to increase throughout the verbal retrieval interval in channels except for ch7, whereas $R_i(k)$ decreases significantly at 100 s in ch7. Moreover, the averages of the dynamic range for BA46 (right), BA10, and BA46 (left) were 1.08, 0.96, and 0.90 m(mol/l)mm, respectively. In Fig. 12, the tendency of $R_i(k)$ to increase after the beginning and subsequently decrease is observed in all channels. The average dynamic ranges for BA46 (right), BA10, and BA46 (left) were 0.74, 0.75, and 0.90 m(mol/l)mm, respectively.

B. DISCRIMINATION RESULTS BY kNN AND SVM

Table 1 lists the results for parameters *TP*, *TN*, *FP*, and *FN* obtained via cross-validation for $k_{nn} = 1, 3, 5$, and 10. The rows list the actual types of memory retrieval and the columns the discriminated types of memory retrieval obtained using our method. The *Accuracy*, *PPV*, and *NPV* are also listed in each table. In Table 1, cases (a), that is, the cases of $k_{nn} = 1$ because all test data are correctly discriminated, *TP* and $TN = 20$, whereas $FP = FN = 0$. Hence, $Accuracy = 1$, $PPV = 1$, and $NPV = 1$. Similarly, in cases (b), (c), and (d), all test data are correctly discriminated. There was no difference in *Accuracy*, *PPV*, and *NPV* between $k_{nn} = 1, 3, 5$, and 10.

TABLE 1. Confusion matrices and overall *Accuracy*, *PPV*, and *NPV* for kNN.

(a) $k_{nn} = 1$

		Discriminated types of memory retrieval by kNN	
		Verbal	Visuospatial
Actual types of memory retrieval	Verbal	$TP = 20$	$FN = 0$
	Visuospatial	$FP = 0$	$TN = 20$

$Accuracy = 1$, $PPV = 1$, $NPV = 1$.

(b) $k_{nn} = 3$

		Discriminated types of memory retrieval by kNN	
		Verbal	Visuospatial
Actual types of memory retrieval	Verbal	$TP = 20$	$FN = 0$
	Visuospatial	$FP = 0$	$TN = 20$

$Accuracy = 1$, $PPV = 1$, $NPV = 1$.

(c) knn = 5

		Discriminated types of memory retrieval by kNN	
		Verbal	Visuospatial
Actual types of memory retrieval	Verbal	$TP = 20$	$FN = 0$
	Visuospatial	$FP = 0$	$TN = 20$

$Accuracy = 1$, $PPV = 1$, $NPV = 1$.

(d) $k_{nn} = 10$

		Discriminated types of memory retrieval by kNN	
		Verbal	Visuospatial
Actual types of memory retrieval	Verbal	$TP = 20$	$FN = 0$
	Visuospatial	$FP = 0$	$TN = 20$

$Accuracy = 1$, $PPV = 1$, $NPV = 1$.

Table 2 lists the results for parameters *TP*, *TN*, *FP*, and *FN* obtained via cross-validation for four kernels: (a) linear kernel, (b) quadratic kernel, (c) polynomial kernel, and (d) Gaussian kernel. In Table 1, for cases (a) and (c), that is, for the linear and polynomial kernels, respectively, TP and TN = 20 because all test data are correctly discriminated, whereas FP = FN = 0. Hence, Accuracy = 1, PPV = 1, and NPV = 1. In Table 2, case (b), that is, for the quadratic kernel, TP = 20 and FN = 0 because all the test data whose actual type of memory retrieval is verbal are correctly discriminated. For visuospatial memory retrieval, 18 of the 20 test datasets were correctly discriminated, and two test datasets were wrongly discriminated; TN = 18 and FP = 2. Hence, for the quadratic kernel, Accuracy = 0.95, PPV = 0.91, and NPV = 1. With regard to Table 2, case (d), which corresponds to the Gaussian kernel, TP = 20 and FN = 0 because all the test data whose actual type of memory retrieval is verbal are correctly discriminated. For visuospatial memory retrieval, 16 of 20 test datasets were correctly discriminated, and 4 test datasets were wrongly discriminated: TN = 16 and FP = 4. Hence, for the quadratic kernel, Accuracy = 0.9, PPV = 0.83, and NPV = 1. Therefore, when the linear or polynomial kernel is applied to the SVM, Accuracy and PPV are higher than the corresponding values of the quadratic or Gaussian kernels.

From Table 1, verbal and visuospatial memory retrieval can be discriminated with high accuracy. Therefore, to validate the SVM contribution to the discrimination results, the discrimination spaces generated by each kernel were compared. In this experiment because 10 indices S_i ($i = 1, 2, \ldots, 10$) were applied to the SVM, the number of dimensions of the discrimination space is 10, which cannot be visually plotted. Hence, the two-dimensional (2D) discrimination space generated by two indices for visualization were compared. Here, S_1 and S_{10} are considered as the two indices. Indices S_1 and S_{10} are calculated from the blood volume measured at ch1 (right BA46) and ch10 (left BA46), which are located farthest apart from each other among all channels. As shown in Figs. 7 and 8 because the blood volumes in the right BA46 and left BA46 regions during the memory retrieval period exhibit different characteristics, S_1 and S_{10} are strongly considered to affect the SVM discrimination results. Hence, the 2D discrimination space is compared using S_1 and S_{10}. Figs. 13(a)–13(d) show the 2D discrimination spaces of the linear, quadratic, polynomial, and Gaussian kernels, respectively. In Fig. 13, the symbols $*$ and ■ denote verbal memory retrieval data and visuospatial memory retrieval data, respectively, and the black dotted line represents the hyperplane that discriminates between the verbal and visuospatial memory retrieval areas. The hyperplanes are generated from the 38 training datasets, and the two test datasets are discriminated. As shown in Figs. 13(a)–13(d), the hyperplanes clearly divide the verbal memory retrieval and visuospatial memory retrieval regions, and both test data are correctly discriminated for all kernels. Thus, we conclude that memory retrieval can be correctly discriminated by both kNN and SVM.

V. DISCUSSION

The loop and visuospatial sketchpad are indispensable components of verbal and visuospatial working memory, respectively. Because the phonological loop is located near the cortex in the Sylvian fissure, the insular cortex in the temporal lobe, supramarginal gyrus, and Broca's area, which are primarily located in the frontal lobe, brain activation in the prefrontal lobe increases markedly during verbal memory retrieval, and our proposed activation index becomes large. In contrast because the visuospatial sketchpad is located in the temporal, parietal, and occipital lobes, the prefrontal lobe is relatively quiescent during visuospatial memory retrieval, and our proposed index is small. Hence, our results indicate that the index defined in (2) discriminated between verbal and visuospatial memory retrieval with great accuracy, independent of the discrimination methods used.

Because there are no existing studies on discriminating between verbal and visuospatial retrieval, a direct comparison with existing methods is not feasible. However, from the cerebral blood volume compiled in [33]–[36], it appears that the existing studies report discrimination accuracies ranging from 0.557 to 0.966 for the other task discrimination (excluding verbal and visuospatial retrieval). In this study,

TABLE 2. Confusion matrices and overall *Accuracy*, *PPV*, and *NPV* for each kernel.

(a) Linear kernel

		Discriminated types of memory retrieval by SVM	
		Verbal	Visuospatial
Actual types of memory retrieval	Verbal	$TP = 20$	$FN = 0$
	Visuospatial	$FP = 0$	$TN = 20$

$Accuracy = 1$, $PPV = 1$, $NPV = 1$.

(b) Quadratic kernel

		Discriminated types of memory retrieval by SVM	
		Verbal	Visuospatial
Actual types of memory retrieval	Verbal	$TP = 20$	$FN = 0$
	Visuospatial	$FP = 2$	$TN = 18$

$Accuracy = 0.95$, $PPV = 0.91$, $NPV = 1$

(c) Polynomial kernel

		Discriminated types of memory retrieval by SVM	
		Verbal	Visuospatial
Actual types of memory retrieval	Verbal	$TP = 20$	$FN = 0$
	Visuospatial	$FP = 0$	$TN = 20$

$Accuracy = 1$, $PPV = 1$, $NPV = 1$.

(d) Gaussian kernel

		Discriminated types of memory retrieval by SVM	
		Verbal	Visuospatial
Actual types of memory retrieval	Verbal	$TP = 20$	$FN = 0$
	Visuospatial	$FP = 4$	$TN = 16$

$Accuracy = 0.9$, $PPV = 0.83$, $NPV = 1$

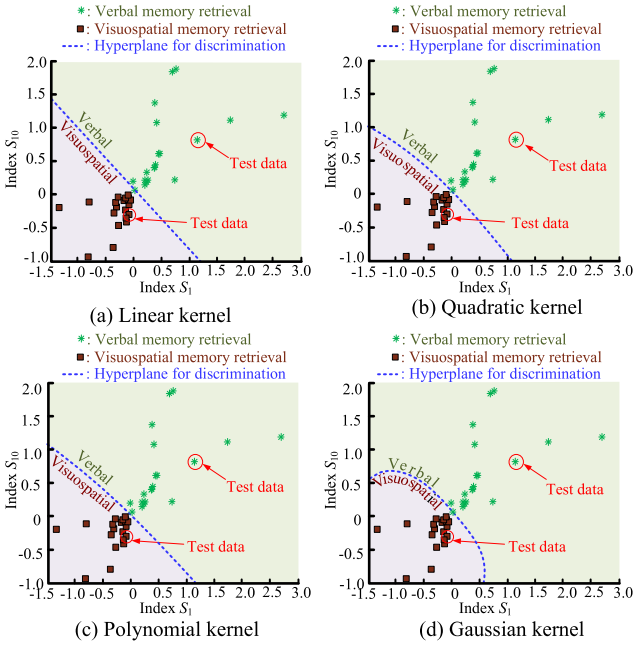

FIGURE 13. Discrimination space generated by indices S_1 and S_{10} for each kernel. The symbols ∗ and ■, and the dotted line represent verbal memory retrieval data and visuospatial memory retrieval data, and the hyperplane, respectively. The hyperplane clearly divides the verbal memory retrieval and visuospatial memory retrieval zones. Hence, both test data are correctly discriminated for all kernels.

an accuracy of one was achieved, which could be interpreted as an encouraging result.

Furthermore, among the fNIRS-based classification methods compiled in [35], [36], the most frequent feature was the mean value. To analyze the novelty and improvement of the proposed method, the performance was evaluated using the same dataset by setting mean values as the features instead of the dynamic range used in our proposed method. As for the SVM, *Accuracy*, *PPV*, and *NPV* were 0.60, 0.60, and 0.60 for (a) linear kernel; 0.68, 0.62, and 0.82 for (b) quadratic kernel; 0.63, 0.58, and 0.78 for (c) polynomial kernel; and 0.75, 0.73, and 0.78 for (d) Gaussian kernel. As for kNN, *Accuracy*, *PPV*, and *NPV* were 0.53, 0.52, 0.57 for $k_{nn} = 1$; 0.60, 0.56, 0.75 for $k_{nn} = 3$; 0.53, 0.51, 0.60 for $k_{nn} = 5$; and 0.50, 0.50, 0.50 for $k_{nn} = 10$. The experimental results show that the dynamic range is appropriate for verbal and non-verbal retrieval discrimination.

In the evaluation experiment for verbal retrieval, the trials were set with different initial letters lasting for 20 s each. The effects of different initial letters and duration among the trials are still open questions. Our future work will elucidate these dependencies. Furthermore, for the features used in the discrimination methods, 10 indices were obtained, $S_1, S_2, \ldots, S_{10}$, which were calculated for all 10 channels observed. The features from the 10 channels were used for classification. It is possible to reduce the number of features, which is also one of our future projects.

VI. CONCLUSION

In this study, a method that can discriminate between verbal and visuospatial memory retrieval was described by using prefrontal blood volume. We used fNIRS to evaluate brain activity while participants retrieved memories, and an index that used fNIRS signals to reflect the type of memory retrieval process was defined. The index was used in a kNN classifier or SVM that discriminated between verbal and visuospatial memory retrieval. As a result, for all $k_{nn} = 1, 3, 5$, and 10 for the kNN and for both the linear and polynomial kernels for the SVM, the values of *Accuracy*, *PPV*, and *NPV* were 1.

Our experimental results indicate that this method may be applied to fields such as education (to develop suitable teaching materials or customize teaching) and neuromarketing. One topic for our future work includes the evaluation of the perfect-pitch teaching method for children.

AUTHOR CONTRIBUTION STATEMENT

Y. Kurihara and T. Matsumoto conceived and designed the experiments. T. Kaburagi acquired the data, T. Kaburagi, K. Nishio, Y. Hamada, and S. Kumagai analyzed and interpreted the data; Y. Kurihara wrote the paper and drafted the article. All authors equally critically revised the manuscript for important intellectual content.

ACKNOWLEDGMENT

The authors would like to thank Editage (www.editage.com) for English language editing.

REFERENCES

[1] A. D. Baddeley and G. J. Hitch, "Working memory," in *Recent Advances in Learning and Motivation*, vol. 8, G. A. Bower, Ed. New York, NY, USA: Academic, 1974, pp. 47–89.
[2] A. D. Baddeley, *Working Memory*. New York, NY, USA: Oxford Univ. Press, 1986.
[3] A. D. Baddeley, "Working memory," *Science*, vol. 255, no. 5044, pp. 556–559, Jan. 1992.
[4] A. Baddeley, "The episodic buffer: A new component of working memory?" *Trends Cognit. Sci.*, vol. 4, no. 11, pp. 417–423, Nov. 2000.
[5] A. D. Baddeley, "Is working memory still working?" *Eur. Psychol.*, vol. 7, no. 2, pp. 85–97, Jun. 2002.
[6] M. Osaka, Y. Nishizaki, M. Komori, and N. Osaka, "Effect of focus on verbal working memory: Critical role of the focus word in reading," *Memory Cognition*, vol. 30, no. 4, pp. 562–571, Jun. 2002.
[7] N. Osaka and M. Osaka, "Individual differences in working memory during reading with and without parafoveal information: A moving-window study," *Amer. J. Psychol.*, vol. 115, no. 4, pp. 501–513, 2002.
[8] G. A. Miller, "The magical number seven, plus or minus two: Some limits on our capacity for processing information," *Psychol. Rev.*, vol. 63, no. 2, pp. 81–97, 1956.
[9] N. Cowan, "The magical number 4 in short-term memory: A reconsideration of mental storage capacity," *Behav. Brain Sci.*, vol. 24, no. 1, pp. 87–114, 2001.
[10] R. Jackendoff, *Foundations of Language: Brain, Meaning, Grammar, Evolution*. Oxford, U.K.: Oxford Univ. Press, 2002.
[11] M. Osaka, N. Osaka, H. Kondo, M. Morishita, H. Fukuyama, T. Aso, and H. Shibasaki, "The neural basis of individual differences in working memory capacity: An fMRI study," *NeuroImage*, vol. 18, no. 3, pp. 789–797, Mar. 2003.
[12] N. Osaka, M. Osaka, H. Kondo, M. Morishita, H. Fukuyama, and H. Shibasaki, "The neural basis of executive function in working memory: An fMRI study based on individual differences," *NeuroImage*, vol. 21, no. 2, pp. 623–631, Feb. 2004.
[13] H. Kondo, M. Morishita, N. Osaka, M. Osaka, H. Fukuyama, and H. Shibasaki, "Functional roles of the cingulo-frontal network in performance on working memory," *NeuroImage*, vol. 21, no. 1, pp. 2–14, Jan. 2004.
[14] K. D. Federmeier, M. Kutas, and R. Schul, "Age-related and individual differences in the use of prediction during language comprehension," *Brain Lang.*, vol. 115, no. 3, pp. 149–161, Dec. 2010.
[15] K. Kahlaoui, V. Vlasblom, F. Lesage, N. Senhadji, H. Benali, and Y. Joanette, "Semantic processing of words in the aging brain: A near-infrared spectroscopy (NIRS) study," *Brain Lang.*, vol. 1, no. 103, pp. 144–145, 2007.
[16] K. Lidzba, E. Schwilling, W. Grodd, I. Krägeloh-Mann, and M. Wilke, "Language comprehension vs. Language production: Age effects on fMRI activation," *Brain Lang.*, vol. 119, no. 1, pp. 6–15, Oct. 2011.
[17] K. Kahlaoui, G. D. Sante, J. Barbeau, M. Maheux, F. Lesage, B. Ska, and Y. Joanette, "Contribution of NIRS to the study of prefrontal cortex for verbal fluency in aging," *Brain Lang.*, vol. 121, no. 2, pp. 164–173, May 2012.
[18] I. Kovelman, M. H. Shalinsky, K. S. White, S. N. Schmitt, M. S. Berens, N. Paymer, and L.-A. Petitto, "Dual language use in sign-speech bimodal bilinguals: FNIRS brain-imaging evidence," *Brain Lang.*, vol. 109, nos. 2–3, pp. 112–123, May 2009.
[19] A. E. Hernandez, "Language switching in the bilingual brain: What's next?" *Brain Lang.*, vol. 109, nos. 2–3, pp. 133–140, May 2009.
[20] R. I. Mayberry, J.-K. Chen, P. Witcher, and D. Klein, "Age of acquisition effects on the functional organization of language in the adult brain," *Brain Lang.*, vol. 119, no. 1, pp. 16–29, Oct. 2011.
[21] L. C. Scherer, R. P. Fonseca, M. Amiri, D. Adrover-Roig, K. Marcotte, F. Giroux, N. Senhadji, H. Benali, F. Lesage, and A. I. Ansaldo, "Syntactic processing in bilinguals: An fNIRS study," *Brain Lang.*, vol. 121, no. 2, pp. 144–151, May 2012.
[22] L. A. Petitto, M. S. Berens, I. Kovelman, M. H. Dubins, K. Jasinska, and M. Shalinsky, "The 'perceptual wedge' hypothesis-as the basis for bilingual babies' phonetic processing advantage: New insights from fNIRS brain imaging," *Brain Lang.*, vol. 121, no. 2, pp. 130–143, May 2012.
[23] K. Timmer, N. Vahid-Gharavi, and N. O. Schiller, "Reading aloud in persian: ERP evidence for an early locus of the masked onset priming effect," *Brain Lang.*, vol. 122, no. 1, pp. 34–41, Jul. 2012.
[24] K. Veroude, D. G. Norris, E. Shumskaya, M. Gullberg, and P. Indefrey, "Functional connectivity between brain regions involved in learning words of a new language," *Brain Lang.*, vol. 113, no. 1, pp. 21–27, Apr. 2010.
[25] K. Stromswold, D. Caplan, N. Alpert, and S. Rauch, "Localization of syntactic comprehension by positron emission tomography," *Brain Lang.*, vol. 52, no. 3, pp. 452–473, Mar. 1996.
[26] M. J. Herrmann, A.-C. Ehlis, and A. J. Fallgatter, "Frontal activation during a verbal-fluency task as measured by near-infrared spectroscopy," *Brain Res. Bull.*, vol. 61, no. 1, pp. 51–56, Jun. 2003.
[27] C.-J. Huang, P.-H. Chou, H.-L. Wei, and C.-W. Sun, "Functional connectivity during phonemic and semantic verbal fluency test: A multichannel near infrared spectroscopy study," *IEEE J. Sel. Topics Quantum Electron.*, vol. 22, no. 3, pp. 43–48, May 2016, doi: 10.1109/JSTQE.2015.2503318.
[28] H. Ayaz, P. A. Shewokis, A. Curtin, M. Izzetoglu, K. Izzetoglu, and B. Onaral, "Using MazeSuite and functional near infrared spectroscopy to study learning in spatial navigation," *J. Visualized Exp.*, no. 56, p. e3443, Oct. 2011, doi: 10.3791/3443.
[29] T. Nakahachi, R. Ishii, M. Iwase, L. Canuet, H. Takahashi, R. Kurimoto, K. Ikezawa, M. Azechi, O. Kajimoto, and M. Takeda, "Frontal cortex activation associated with speeded processing of visuospatial working memory revealed by multichannel near-infrared spectroscopy during advanced trail making test performance," *Behavioural Brain Res.*, vol. 215, no. 1, pp. 21–27, Dec. 2010, doi: 10.1016/j.bbr.2010.06.016.
[30] R. McKendrick, H. Ayaz, R. Olmstead, and R. Parasuraman, "Enhancing dual-task performance with verbal and spatial working memory training: Continuous monitoring of cerebral hemodynamics with NIRS," *NeuroImage*, vol. 85, pp. 1014–1026, Jan. 2014, doi: 10.1016/j.neuroimage.2013.05.103.
[31] R. Sitaram, N. Weiskopf, A. Caria, R. Veit, M. Erb, and N. Birbaumer, "FMRI brain-computer interfaces," *IEEE Signal Process. Mag.*, vol. 25, no. 1, pp. 95–106, Jan. 2008, doi: 10.1109/MSP.2008.4408446.
[32] K. Watanabe, H. Tanaka, K. Takahashi, Y. Niimura, K. Watanabe, and Y. Kurihara, "NIRS-based language learning BCI system," *IEEE Sensors J.*, vol. 16, no. 8, pp. 2726–2734, Apr. 2016.
[33] N. Naseer and K.-S. Hong, "Classification of functional near-infrared spectroscopy signals corresponding to the right- and left-wrist motor imagery for development of a brain–computer interface," *Neurosci. Lett.*, vol. 553, pp. 84–89, Oct. 2013.
[34] N. Naseer, M. J. Hong, and K.-S. Hong, "Online binary decision decoding using functional near-infrared spectroscopy for the development of brain–computer interface," *Exp. Brain Res.*, vol. 232, no. 2, pp. 555–564, Nov. 2013.
[35] N. Naseer and K.-S. Hong, "FNIRS-based brain-computer interfaces: A review," *Frontiers Hum. Neurosci.*, vol. 9, p. 3, Jan. 2015.
[36] K.-S. Hong, M. J. Khan, and M. J. Hong, "Feature extraction and classification methods for hybrid fNIRS-EEG brain-computer interfaces," *Frontiers Hum. Neurosci.*, vol. 12, p. 246, Jun. 2018.
[37] M. D. Lezak, *Neuropsychological Assessment*, 3rd ed. Oxford, U.K.: Oxford Univ. Press, 1995.
[38] E. M. Weiss, C. Siedentopf, A. Hofer, E. A. Deisenhammer, M. J. Hoptman, C. Kremser, S. Golaszewski, S. Felber, W. W. Fleischhacker, and M. Delazer, "Brain activation pattern during a verbal fluency test in healthy male and female volunteers: A functional magnetic resonance imaging study," *Neurosci. Lett.*, vol. 352, no. 3, pp. 191–194, Dec. 2003.
[39] S. Abrahams, L. H. Goldstein, A. Simmons, M. J. Brammer, S. C. R. Williams, V. P. Giampietro, C. M. Andrew, and P. N. Leigh, "Functional magnetic resonance imaging of verbal fluency and confrontation naming using compressed image acquisition to permit overt responses," *Hum. Brain Mapping*, vol. 20, no. 1, pp. 29–40, Sep. 2003.
[40] S. Wagner, A. Sebastian, K. Lieb, O. Tüscher, and A. Tadić, "A coordinate-based ALE functional MRI meta-analysis of brain activation during verbal fluency tasks in healthy control subjects," *BMC Neurosci.*, vol. 15, no. 1, p. 19, Jan. 2014.
[41] C.-E.-J. Tseng, S. Froudist-Walsh, J. Kroll, V. Karolis, P. J. Brittain, N. Palamin, H. Clifton, S. J. Counsell, S. C. R. Williams, R. M. Murray, and C. Nosarti, "Verbal fluency is affected by altered brain lateralization in adults who were born very preterm," *Eneuro*, vol. 6, no. 2, pp. 1–16, Mar. 2019, doi: 10.1523/ENEURO.0274-18.2018.

[42] J.-J. Sun, X.-M. Liu, C.-Y. Shen, X.-Q. Zhang, G.-X. Sun, K. Feng, B. Xu, X.-J. Ren, X.-Y. Ma, and P.-Z. Liu, "Reduced prefrontal activation during verbal fluency task in chronic insomnia disorder: A multichannel near-infrared spectroscopy study," *Neuropsychiatric Disease Treatment*, vol. 13, pp. 1723–1731, Jun. 2017.
[43] M. Meinzer, L. Seeds, T. Flaisch, S. Harnish, M. L. Cohen, K. McGregor, T. Conway, M. Benjamin, and B. Crosson, "Impact of changed positive and negative task-related brain activity on word-retrieval in aging," *Neurobiol. Aging*, vol. 33, no. 4, pp. 656–669, Apr. 2012.
[44] A. Rey, "The psychological examination in cases of traumatic encephalopathy. Problems," *Arch. de Psychologie*, vol. 28, pp. 286–340, Jan. 1941.
[45] M. Notoya, K. Inoue, A. Hirabayashi, K. Sakamoto, C. Sasaguchi, and M. Toyama, "A comparison of rey-osterrieth complex figure test scores: With/without mouthpiece and with/without noise," *World J. Neurosci.*, vol. 7, no. 3, pp. 282–292, 2017.
[46] A. L. Zaninotto, J. E. Vicentini, D. J. F. Solla, T. T. Silva, V. M. D. P. Guirado, F. Feltrin, M. C. S. de Lucia, M. J. Teixeira, and W. S. Paiva, "Visuospatial memory improvement in patients with diffuse axonal injury (DAI): A 1-year follow-up study," *Acta Neuropsychiatrica*, vol. 29, no. 1, pp. 35–42, Feb. 2017.
[47] G. J. Hyun, J. W. Park, J. H. Kim, K. J. Min, Y. S. Lee, S. M. Kim, and D. H. Han, "Visuospatial working memory assessment using a digital tablet in adolescents with attention deficit hyperactivity disorder," *Comput. Methods Programs Biomed.*, vol. 157, pp. 137–143, Apr. 2018.
[48] M. Klojčnik, V. Kavcic, and K. Bakracevic Vukman, "Relationship of depression with executive functions and visuospatial memory in elderly," *Int. J. Aging Hum. Develop.*, vol. 85, no. 4, pp. 490–503, Dec. 2017.
[49] P. Chen, A. J. Hartman, C. Priscilla Galarza, and J. DeLuca, "Global processing training to improve visuospatial memory deficits after right-brain stroke," *Arch. Clin. Neuropsychol.*, vol. 27, no. 8, pp. 891–905, Oct. 2012.
[50] R. Human, K. G. Thomas, A. Dreyer, A. R. Amod, P. S. Wolf, and W. J. Jacobs, "Acute psychosocial stress enhances visuospatial memory in healthy males," *South Afr. J. Psychol.*, vol. 43, no. 3, pp. 300–313, Sep. 2013.
[51] M.-S. Kim, Y. Namgoong, and T. Youn, "Effect of organizational strategy on visual memory in patients with schizophrenia," *Psychiatry Clin. Neurosci.*, vol. 62, no. 4, pp. 427–434, Aug. 2008.

YOSUKE KURIHARA (Member, IEEE) received the M.E. and Ph.D. degrees from Hosei University, Tokyo, in 2003 and 2009, respectively.

He joined Hitachi Software Engineering Ltd., in 2003. From 2009 to 2012, he served as an Assistant Professor for Seikei University. From 2013 to 2018, he was an Associate Professor with Aoyama Gakuin University, where he has been serving as a Professor, since 2019. He is the author of five books, more than 70 journal articles, and more than 100 international conference proceedings, and he holds four patents. His research interests include system engineering, sensing methods, biosensing, and system information engineering.

Dr. Kurihara is a member of the Japanese Society for Medical and Biological Engineering, the Society of Instrument and Control Engineers, the Electrical Engineers of Japan, and the Japan Society for Fuzzy Theory and Intelligent Informatics.

TAKASHI KABURAGI (Member, IEEE) received the B.E., M.E., and Ph.D. degrees from Waseda University, in 2003, 2005, and 2009, respectively.

He is currently an Instructor with the College of Liberal Arts, International Christian University, where he has been a Faculty Member, since 2019. His research interests include machine learning and time series data analysis.

KEITA NISHIO received the B.E. degree from Aoyama Gakuin University, in 2019, where he is currently pursuing the master's degree with the Graduate School of Science and Engineering, Aoyama Gakuin University.

His research interests include bio-signal processing and machine learning.

YURI HAMADA (Member, IEEE) received the B.S., M.S., and Ph.D. degrees in engineering from Chuo University, Japan, in 2008, 2010, and 2017, respectively. From 2018 to 2020, she served as an Assistant Professor for Chuo University. Since 2020, she has been an Assistant Professor in Industrial and Systems Engineering with Aoyama Gakuin University. Her research interests include the modeling of communication processes and analysis of decision making processes. She is a member of Japan Society of Kansei Engineering and Japanese Cognitive Science Society.

TOSHIYUKI MATSUMOTO received the M.E. and Ph.D. degrees from Keio University, Tokyo, in 1987 and 2001, respectively.

From 2003 to 2010, he served as an Associate Professor for Aoyama Gakuin University, where he has been serving as a Professor, since 2011. His research interests include industrial engineering, improvement (KAIZEN) activities, production systems design, and manufacturing education systems.

Dr. Matsumoto is a member of the Japan Industrial Management Association.

SATOSHI KUMAGAI received the B.E. and M.E. degrees from Keio University, in 1984 and 1986, respectively, and the Ph.D. degree from Sophia University, in 2000.

He is currently a Professor with the College of Science and Engineering, Aoyama Gakuin University, where he has been a Faculty Member, since 2010. His research interests include the areas of management systems and business process modeling.